Aerospace Science and Technology ••• (••••) •••–•••

Contents lists available at ScienceDirect

Aerospace Science and Technology

www.elsevier.com/locate/aescte

Instability detection of centrifugal compressors by means of acoustic measurements

Zhenzhong Sun, Wangzhi Zou, Xinqian Zheng

Turbomachinery Laboratory, State Key Laboratory of Automotive Safety and Energy, Tsinghua University, Beijing, 100084, China

ARTICLE INFO

Article history:
Received 3 June 2018
Received in revised form 4 August 2018
Accepted 4 September 2018
Available online xxxx

Keywords:
Centrifugal compressor
Instability
Acoustic measurement
Stall
Surge
Vaneless diffuser

ABSTRACT

Preventing the compressor from instability phenomena is of great importance for the safe operation of many industrial products, such as aero-engines. Hence, a simple and low-cost method is extremely demanded to detect instability phenomena of compressors, especially in the real operating environment, and acoustic measurement is an alternative solution. In this paper, dynamic pressure and acoustic characteristic of a centrifugal compressor are experimentally investigated. First, all typical operation conditions of the compressor are illustrated and all instability phenomena that occur within the compressor are identified. Then, dynamic pressure is analyzed to present characteristics of different instability phenomena. Finally, the ability of acoustic measurement to detect instability phenomena is discussed with detailed analysis on acoustic signals, and guidelines for instability detection by means of acoustic measurement are established. Results show that four instability phenomena, rotating instability, rotating stall, mild surge and deep surge, occur within the compressor. In addition, the acoustic sensor is recommended to be installed near the compressor casing, and the acoustic signal can detect the rotating stall, the mild surge and the deep surge by capturing their characteristic frequency. This paper demonstrates the ability to capture instability phenomena via acoustic signals and provides an acoustic measurement technology to detect instabilities at any time of the full life cycle of a compressor.

1. Introduction

Compressors are widely applied in industry, transportation and power system. However, the performance of a compressor itself is limited by instability phenomena, which significantly affects the stable flow range and damages the compressor components. Therefore, detecting and avoiding instability phenomena are significant for the application of compressors.

With differences in time and length scale, instability in compressors mainly includes three groups, rotating instability, rotating stall and surge [1]. Rotating instability is characterized by broadband frequency spectrum [1,2] and is closely related to the formation and movement of the vortex near the leading edge plane which is formed by interactions among the tip-clearance flow, axially reversed endwall flow and the incoming flow [3]. The time scale and length scale of rotating instability are at the order of the blade passing frequency (*BPF*) and the compressor blade pitch, respectively [4].

As an internal compressor instability, rotating stall is usually related to flow separations, and its time scale is at the order of rotor revolutions whereas its length scale is at the order of compressor circumference [5]. Many researches on rotating stall focus on the stall inception that has two types, one is modal wave type and the other is spike type. These two stall inceptions differ in many aspects, like the time and length scales [6], the oscillation amplitude and the rotational speed. The modal wave type stall inception often occurs at or slightly beyond the peak of the stagnation-to-static pressure rise of the compressor [7], and investigations by Haynes et al. [8] and Paduano et al. [9] show that the rotational speed of modal wave type stall cells is approximately 20% to 50% of the impeller speed. The spike type stall inception is usually characterized by an upward spike in the transient pressure and a downward spike in the velocity [6], and the rotational speed is approximately 50% to 70% of the impeller speed [7]. In addition, the spike type stall inception often occurs at conditions in which the stagnation-to-static pressure rise characteristic has a negative slope [7].

Surge is a global instability of the entire compression system, and the annulus-averaged flow in the system can be observed to oscillate when surge occurs (see Greitzer et al. [10]). The time scale of surge is at the order of Helmholtz frequency of the compression system. According to the occurrence of reverse flow, surge could be further classified into two types, the deep surge with reverse flow and mild surge without reverse flow [11]. Mild surge usu-

E-mail address: zhengxq@tsinghua.edu.cn (X. Zheng).

https://doi.org/10.1016/j.ast.2018.09.006
1270-9638/

Nomenclature

ρ	density
a	sound speed
f_H	Helmholtz frequency
l	equivalent length of the duct
p_r	reference dynamic pressure
s	signal
u	circumferential velocity
A	equivalent cross-sectional area of the duct
BPF	blade passing frequency
DS	deep surge
MS	mild surge
FFT	Fast Fourier Transform
PPF	passage passing frequency of the compressor
V	compressed air volume

Subscripts

0	atmosphere condition
2	trailing edge of the impeller blade
ave	averaged value of a signal
C	compressor
T	turbine

ally occurs at low mass flow rates, but it can also appear at the middle mass flow rate between deep surge and choke [11], and the occurrence of mild surge is often accompanied by minor flow oscillation and reduced efficiency. In contrast, deep surge always emerges with drastic fluctuations in pressure, flow and noise, and it could lead to catastrophic failure of the whole system [12].

To detect and analyze the instability of compressors, many works with different methodologies and instrumentations have been carried out. Li et al. [13] identified stall precursors by analyzing the casing static pressure and outlet total pressure signals. Zheng et al. [14,15] and Sun et al. [16] studied different instability phenomena and the instability evolution by dynamic static pressures and static temperatures measured at different streamwise locations. The hot-wire probe was also used to investigate instability phenomenon. For example, Alone et al. [17] measured the unsteady velocity in the tip region ahead of a rotor at the stall condition. Particle image velocimetry (*PIV*) is another effective method for instability investigation. A recent work has been reported by Brandstetter et al. [18], and the PIV result shows the structure and breakdown of the tip leakage vortex and it is thought to be responsible for the spike-type stall inception. Additionally, computational fluid dynamics (*CFD*) is also used to investigate compressor instabilities [19,20]. Vo et al. [7] established criteria for the spike-type stall inception based on their unsteady simulation results; Pullan et al. [21] described the structures that produce a spike-type route to rotating stall with unsteady simulation, and determined the mechanism of the spike-type stall inception. Recently, Enrico Munari et al. [22] applied the vibro-acoustic analysis to detect the precursor signals of stall and surge for the first time, and underlined the capability and usefulness of accelerometers and microphones for detecting stall and surge.

The literature review gives a simple introduction on instability phenomena of compressors, as well as methods to detect and analyze these instabilities. Nevertheless, most of the introduced methods are either expensive and complex (like dynamic signal measurement or PIV) or time-consuming (like unsteady simulation), and some of them even induce additional disturbance on the flow (like pressure or temperature measurement) or require special manufactures (like PIV). More importantly, most of these methods are only applicable to the laboratory environment, so it is challenging to apply these methods to industrial products, especially in the real operating environment. On the other hand, the instability of a compressor product may be different at different period of the full life cycle due to the performance degradation or change of working condition, and it is of great significance to detect the potential instability to ensure the safe operation of the compressor product. Therefore, a low-cost, simple and flexible method is hugely demanded that can capture as many instability phenomena as possible in a compressor in service, and acoustic measurement seems to be a satisfying solution. In this paper, the instability phenomenon of a centrifugal compressor is investigated by both dynamic pressure measurement and acoustic measurement, and the ability of acoustic signals to capture the instability is analyzed and discussed, thereby providing an alternative way of detecting instability phenomena within compressor in real operating environment.

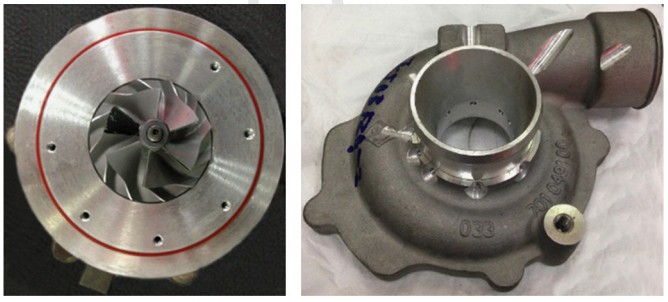

Fig. 1. Picture of the investigated compressor.

Table 1
Geometric parameters of the compressor.

Parameters	Value (unit)
Impeller blade number	6 + 6 (main+splitter)
Impeller outlet diameter	50.00 (mm)
Impeller backsweep angle	38.00 (°)
Inlet hub diameter	11.00 (mm)
Inlet shroud diameter	37.10 (mm)
Diffuser type	vaneless diffuser
Diffuser outlet diameter	84.40 (mm)
Diffuser width	2.65 (mm)

2. Experimental setup

A centrifugal compressor with a vaneless diffuser was experimentally investigated in this study. Shown in Fig. 1 is the photo of main components of the compressor, including the impeller, the back plate, the volute and the casing. More detailed geometric specifications of the compressor are listed in Table 1.

The schematic diagram of the test rig facility is shown in Fig. 2. Besides the centrifugal compressor, the test rig contains the piping system, driving system (including turbine, combustor and connecting pipes) and control system (not shown in Fig. 2). During the experiment, the turbine extracts energy from the high pressure and high temperature gas generated in the combustor and drives the compressor with a required rotating speed. Flow parameters are measured at both inlet and outlet of the compressor. At both the inlet pipe upstream of the compressor and the vertical outlet pipe downstream of the compressor, probes are installed to measure the total pressure and total temperature, and the mass

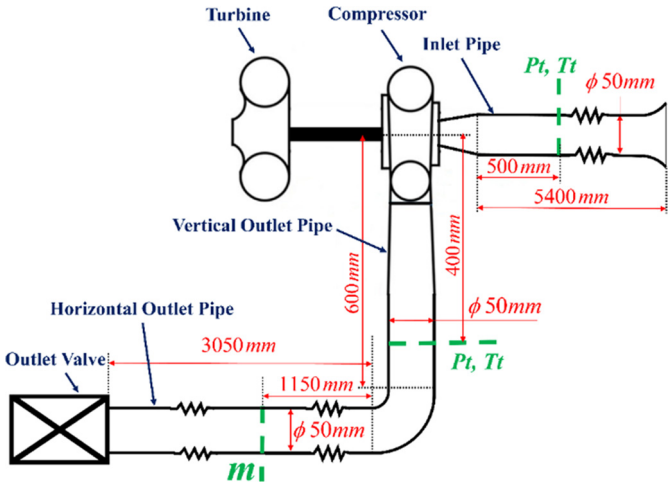

Fig. 2. Schematic diagram of the experimental test rig.

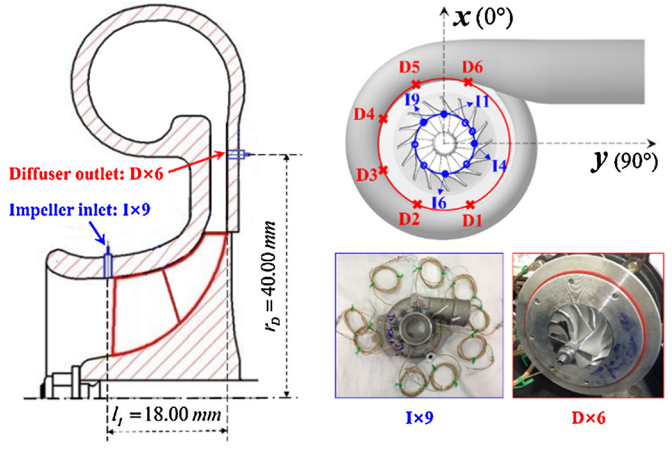

Fig. 3. Layout of dynamic pressure transducer installation.

flow rate is also measured with the flowmeter installed at the horizontal outlet pipe. Additionally, the rotating speed, the ambient pressure together with the ambient temperature are also recorded during the experiment. With those data measured above, the compressor characteristics and performance map could be obtained.

Dynamic measurements were carried out at each tested operation condition with dynamic pressure transducers and acoustic sensors, the former measured the dynamic static pressure near the compressor casing while the latter recorded the acoustic signal around the compressor. Detailed description of the measurement is as follows: The power of the turbine is controlled by adjusting the fuel and air going into the combustor, which ensures the compressor operates at required rotating speed. The operating point of the compressor is adjusted by the downstream outlet valve. For each operating point, only when all the concerned flow parameters, including the mass flow rate, the pressure ratio, the efficiency and the rotating speed, stay within a presupposed small range for 25 seconds, the measurement begins. The pressure measurement and acoustic measurement start and finish simultaneously. At the same time, static flow parameters illustrated in Fig. 2 are also measured and recorded.

The dynamic pressure transducers are produced by *Kulite Semiconductor Products, Inc.* which use a standard miniature silicon diaphragm to obtain extremely high natural frequencies in the smallest thread mount available and their natural frequency is 240 kHz (pressure range of 25 psi) and 300 kHz (pressure range of 50 psi). Two measurement sections, the impeller inlet (marked as "I") and the diffuser outlet (marked as "D") as shown in Fig. 3,

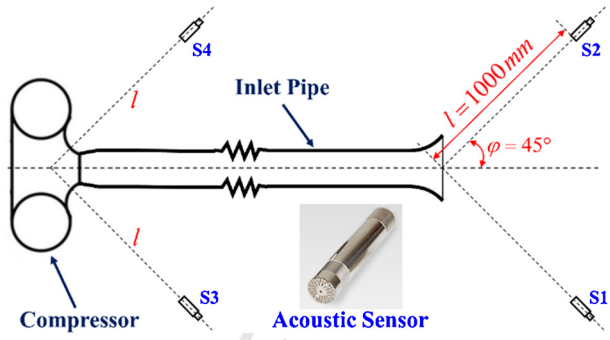

Fig. 4. Top view of the acoustic sensor installation.

Table 2
Technical features of the acoustic sensor.

Parameters	Value
Open-circuit sensitivity	−26 dB ± 2 dB
Frequency response	20 Hz ~ 20 kHz
Dynamic range	>146 dB
Operating temperature	243 K ~ 353 K
Temperature coefficient	−0.012 dB/K

were selected to install the dynamic pressure transducers. Fig. 3 also illustrates the layout of these transducers to show their circumferential installation positions. Nine 25 psi dynamic pressure transducers numbered from I1 to I9 were placed at the impeller inlet. Except for "I3" which located at the middle of "I2" and "I4", the remaining eight transducers were distributed uniformly every 45 degrees. Within the circumferential range from 157.5° to 22.5° (clockwise), six 50 psi dynamic pressure transducers were installed uniformly along the circumferential direction, and these transducers were numbered from D1 to D6.

Four acoustic sensors were placed in the same horizontal plane with the compressor rotating axis, and the top view of the acoustic sensor installation is shown in Fig. 4. These acoustic sensors were named from S1 to S4. S1 and S2 were set up near the inlet pipe entrance, while S3 and S4 were set up near the compressor casing, and the distance between these sensors and the inlet pipe entrance / compressor casing is 1000 millimeters (as shown in Fig. 4). Additionally, the acoustic sensor is the *MP201 microphone* produced by *BSWA TECH* and some of its technical features are listed in Table 2.

3. Analysis on experimental results

The maximum tested rotating speed during the experiment is 200,000 rpm and it is defined as the 100% rotating speed. In addition, the compressor performances at other two lower rotating speeds, 160,000 rpm (80%) and 100,000 rpm (50%), were also investigated, and the three tested rotating speeds represent low, moderate and high rotating speed, respectively. This chapter will analyze and discuss the experimental results, including the steady measurement (performance map), the dynamic pressure measurement and the acoustic measurement. First, the paper presents all typical operation conditions of the compressor and all instability phenomena that occur within the compressor. Then, dynamic pressure signals at each operation condition are analyzed in the frequency domain and/or time domain to present characteristics of different instability phenomena. Finally, acoustic signals are analyzed and their abilities to detect instability are discussed. Additionally, guidelines for instability detection by means of acoustic measurements are established.

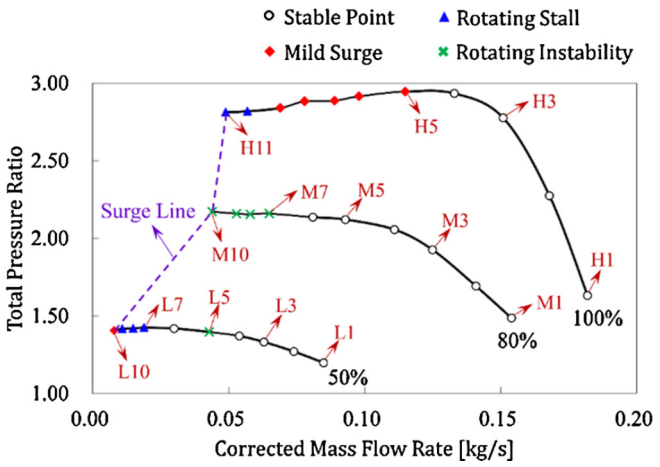

Fig. 5. Performance of the compressor total pressure ratio.

3.1. Compressor performance and pressure characteristics of instability phenomena

The compressor performance in terms of total pressure ratio is shown in Fig. 5. The dash line lying on the left side of the figure denotes the instability boundary beyond which the compressor will suffer deep surge. For the sake of convenience, operation points at each rotating speed are numbered in sequence, as presented in Fig. 5. As can be noticed, with mass flow rate decreases, operation points at low rotating speed (50%) are numbered from "L1" to "L10" ("L" denotes the low rotating speed) one by one, and same rules are applied for operation points at moderate and high rotating speeds. Throughout all operation conditions shown in Fig. 5, the compressor suffers four different instability phenomena: the rotating instability marked with cross, the rotating stall marked with triangle, the mild surge marked with diamond and the deep surge that is not presented in Fig. 5. When operating at different rotating speeds, the compressor experiences different instability phenomena and different evolution process from stable to unstable conditions, especially at high rotating speed where the so-called "two-region surge" phenomenon appears: the compressor successively experiences stable points, mild surge, rotating stall and deep surge.

Those instability phenomena that occur within the compressor can be distinguished and identified on the basis of their unique dynamic characteristics, and dynamic pressure is an alternative and effective tool to help analyze the dynamic characteristics. According to Fig. 5, all four instability phenomena occur at low rotating speed (50%). Thus, following discussions will mainly focus on the low rotating speed.

Take signals recorded by transducer "I7" and "D3" as representatives of the pressure at the impeller inlet and the diffuser outlet, respectively. The frequency characteristics of the dynamic pressure signal at each operation point of low rotating speed are illustrated in Fig. 6, and the figure is obtained by using "Fast Fourier Transform" (*FFT*) to the signal. When the compressor operates at high mass flow rates (L1∼L4), only the passage passing frequency (*PPF*) of the compressor is prominent at both the impeller inlet and the diffuser outlet, thereby indicating that the pressure oscillation inside the compressor is mainly caused by the main blade passing effect. Then rotating instability appears at the impeller inlet when the compressor operates at L5, which is characterized by broadband pressure oscillation. The enlarged view of L5 in Fig. 7 shows the frequency band of the rotating instability is from 24% to 88% of PPF, and the broadband hump is about 46% of PPF. This result is quite similar to the conclusions drawn by Day [1]. Considering that a flow passage contains one main blade and one splitter blade, the blade passing frequency of the compressor (BPF_C) should be two times that of PPF, so the broadband hump of rotating instability is approximately 23% of BPF_C.

According to Fig. 6, a salient frequency of close to 4% PPF appears at operation points L6, L7, L8, L9 and L10. This frequency reveals the rotating stall disturbance. Fig. 8 shows details of this disturbance in time domain, and the ordinate illustrates the dynamic pressure oscillation while abscissa is the time indicator in the unit of rotor revolution. Dynamic pressure signals shown in Fig. 8 are band-pass filtered with band-pass frequency ranging from 1% to 20% PPF, and these pressure signals are recorded at operation point L9. Obvious phase lags can be noticed among different circumferential positions, thereby indicating the rotational effect of stall cells, and the rotational velocity could be calculated to be 65.22% or 25.00% of the impeller speed (as shown in Fig. 8). This demonstrates the occurrence of rotating stall. Considering that the PPF is six times that of impeller frequency, the rotational velocity of stall cells is 10.87% PPF or 4.17% PPF, and neither of them agrees with the frequency of 3.93% PPF. For the dynamic pressure at a certain circumferential position, like "D2" shown in Fig. 8, a periodic oscillation indicates a stall cell, and 15 stall cells are detected within 63.7 rotor revolutions, so the generation frequency of stall cells is about 3.92% PPF, which is quite close to the salient frequency appearing at operation point L9 (3.93% PPF). Therefore, it is summarized that the salient frequency close to 4% PPF in the frequency spectrum reflects the generation frequency of stall cells, and it reveals the occurrence of rotating stall. In addition, this salient frequency also appears at the mild surge condition (L10), thereby indicating that the mild surge disturbance is accompanied by the rotating stall.

The Helmholtz frequency of the compression system plays a significant role in mild surge condition, and its definition is given by Greitzer [23] as follows,

$$f_H = \frac{a}{2\pi} \cdot \sqrt{\frac{A}{l \cdot V}} \tag{1}$$

where a denotes the sound speed, l and A represent the equivalent length and equivalent cross-sectional area of the duct, respectively, and V is the compressed air volume. At the operation point L10, the total temperature measured at the compressor inlet and outlet is 306 K and 358 K respectively, and taking the averaged total temperature (332 K) as the equivalent value, the sound speed is calculated to be 365 m/s. According to the geometric properties of the tested compression system listed in Table 3, the Helmholtz frequency could be obtained by equation (2),

$$f_H = \frac{365}{2 \cdot \pi} \cdot \sqrt{\frac{1}{4609.1 \times 0.0071668}} \approx 10.11\,(\mathrm{Hz}) \tag{2}$$

The pressure signal in time domain of the mild surge disturbance (L10) is shown in Fig. 9, and it is low-pass filtered with a cut-off frequency of 5% PPF. The ordinate scale is at the order of a reference dynamic pressure p_r that is defined in equation (3).

$$p_r = \frac{1}{2} \times \rho_0 \cdot u_2^2 \tag{3}$$

where ρ_0 is the air density of the atmosphere (approximately 1.205 kg/m^3), and u_2 is the impeller tangential velocity at the trailing edge, and it can be calculated that the absolute value of p_r is approximately 41.3 kPa and 165.2 kPa at 50% and 100% rotating speeds, respectively. The mild surge disturbance is analogous to a sinusoidal wave, and within 860 rotor revolutions there are seven mild surge waves, so the frequency of the mild surge is approximately 1.36‰ PPF (13.72 Hz), which is similar to the frequency spectrum result (12.97 Hz according to Fig. 6), and both of them are close to the Helmholtz frequency of the compression system.

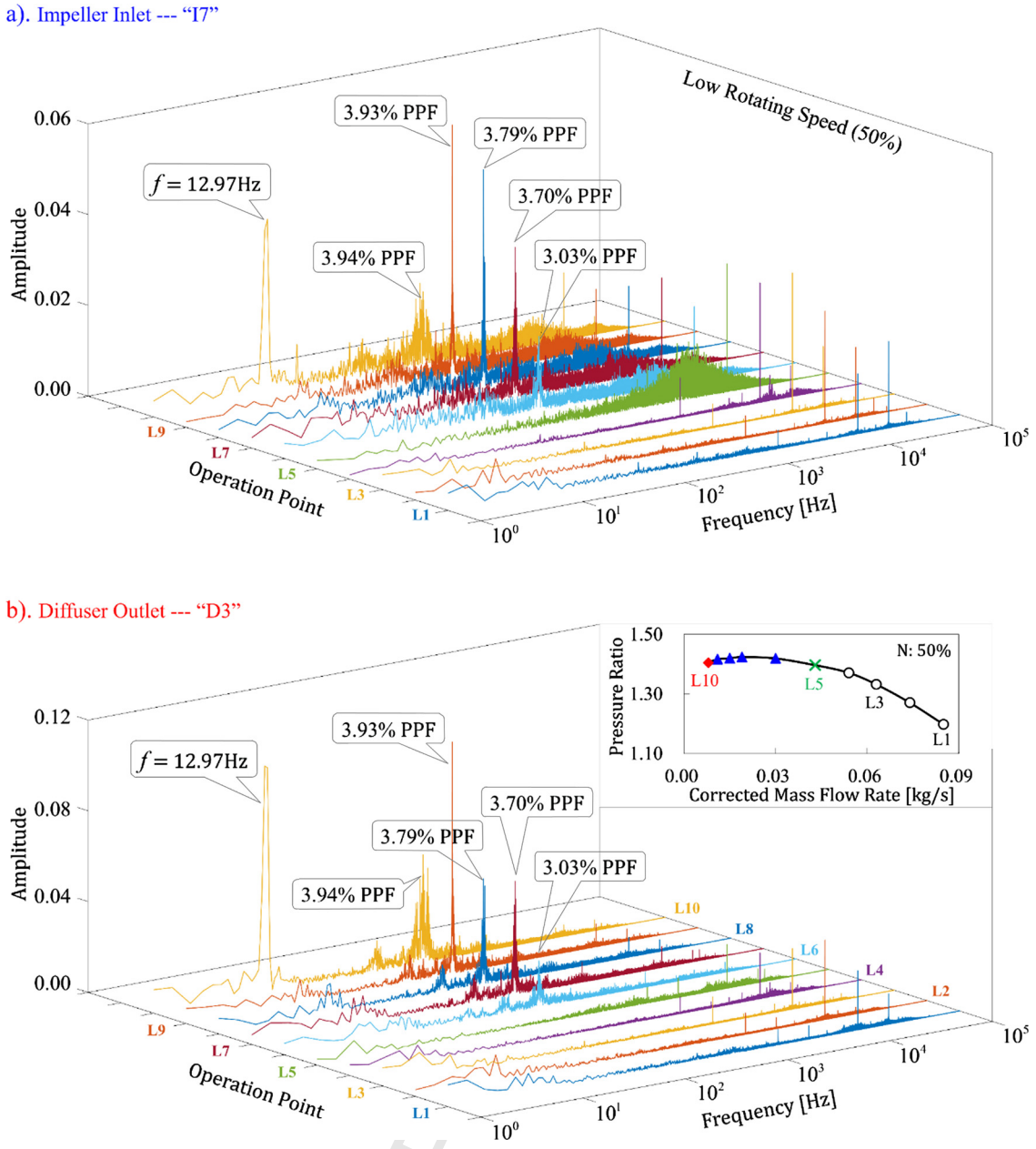

Fig. 6. Frequency characteristics of the pressure signal of a) the impeller inlet ("I7") and b) the diffuser outlet ("D3") at low rotating speed.

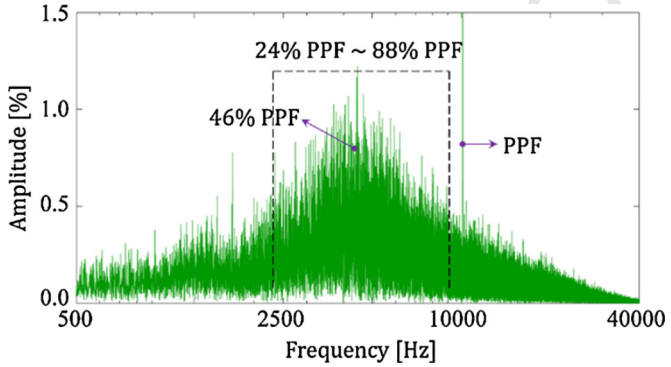

Fig. 7. Enlarged view of frequency characteristic of L5 in Fig. 6(a).

The deep surge condition is easy to be recognized since it is always accompanied with dramatic vibration and discernible noise. Fig. 10 compares pressure characteristics in both frequency domain and time domain between mild surge point (L10) and deep surge conditions (50% speed). The characteristic frequency of deep surge is found to be a little smaller than that of mild surge, whereas amplitude of pressure oscillation is much larger. Unlike that at the mild surge condition at which the pressure oscillates with a wave-like shape, the pressure at deep surge condition oscillates abruptly and presents a leptokurtic waveform. Additionally, Fig. 10(b) also shows that there are five oscillation waves within 753 rotor revolutions, so the frequency of deep surge oscillation could be calcu-

Table 3
Geometric properties of the compression system.

Components	l (mm)	A (mm^2)	V (m^3)	l/A (m^{-1})
Inlet Pipe	5400	1963.5	–	2750.2
Outlet Pipe - V	600	1963.5	0.0011781	305.58
Outlet Pipe - H	3050	1963.5	0.0059887	1553.3
Total	–	–	0.0071668	4609.1

*"- V" means vertical & "- H" means horizontal

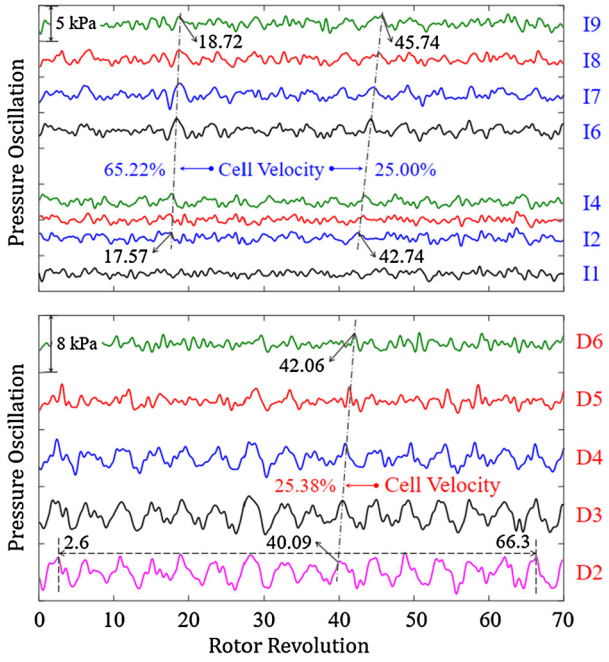

Fig. 8. Pressure oscillation at the impeller inlet at operation point L9.

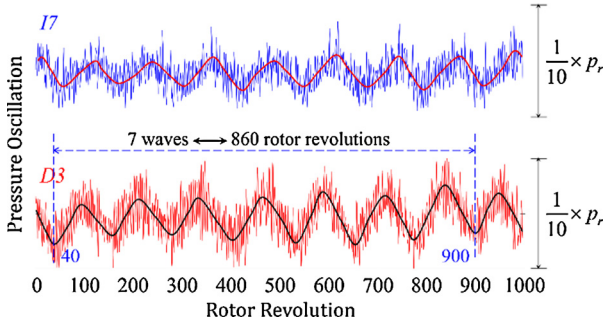

Fig. 9. Pressure signal of mild surge at " L10" recorded by transducers "I7" and "D3".

lated to be 1.11‰ PPF (approximately 11 Hz), which is in agreement with the FFT result.

In summary, the compressor experiences four instability phenomena among all operation conditions: the rotating instability, the rotating stall, the mild surge and the deep surge. The rotating instability is characterized by a broadband oscillation with the broadband hump to be 46% PPF. The rotating stall is characterized by the generation frequency (approximately 4% PPF) of stall cells. The frequency of mild surge is close to the Helmholtz frequency of the compression system and the pressure oscillates with a wave-like shape, while the frequency of deep surge is a little lower than that of mild surge and its pressure oscillates with leptokurtic waveforms.

3.2. Acoustic characteristics of instability phenomena

The compressor performance and the pressure characteristic of instability phenomena have been discussed and analyzed in detail, and this section mainly analyzes the acoustic characteristic and assesses the ability of acoustic signals to detect instability phenomena. Then, guidelines are given to help to detect compressor instability phenomena by means of acoustic measurement.

Similar to the analysis on pressure, operation points with instability phenomena at low rotating speed (50%) are selected to investigate the acoustic signal. Operation point L5 is characterized by rotating instability with broadband oscillations. The frequency

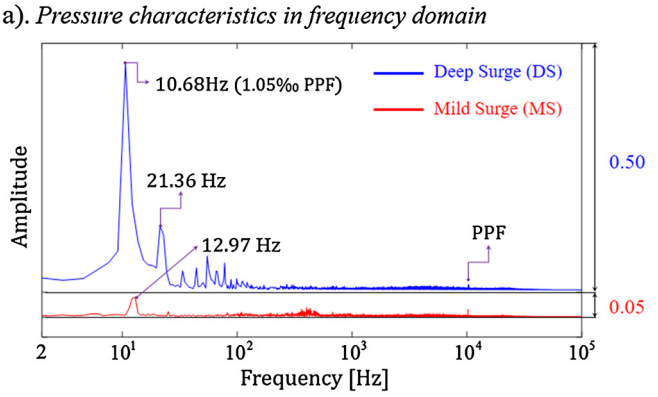

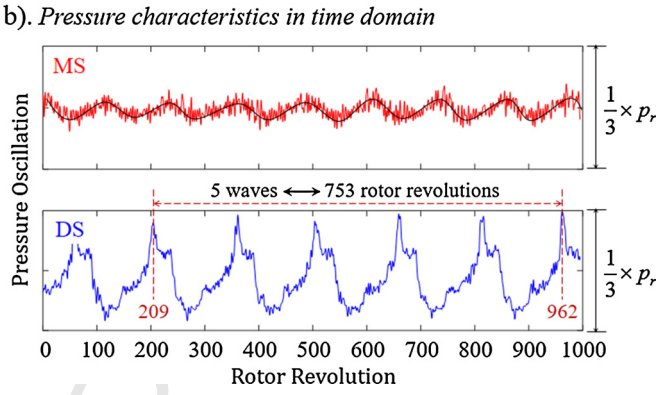

Fig. 10. Pressure characteristics in a) frequency domain and b) time domain at deep surge condition (signal recorded by transducer "I7"). (For interpretation of the references to color in this figure, the reader is referred to the web version of this article.)

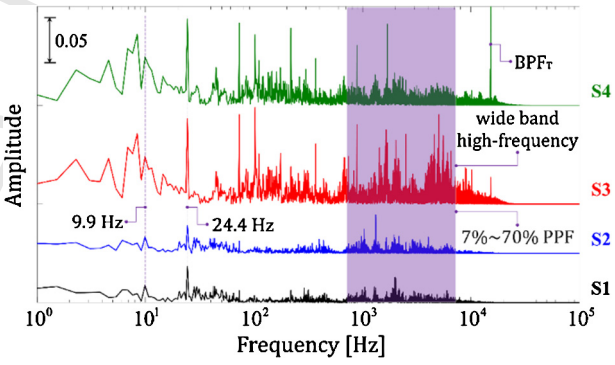

Fig. 11. Frequency characteristic of acoustic signals ("L5").

characteristic of acoustic signals at L5 is illustrated in Fig. 11, from which it can be noticed that acoustic signals contain broadband elements. However, the frequency range is from 7% to 70% PPF, which is different from the pressure signal result (the frequency range is 24% to 88% PPF). According to the analysis, acoustic signals are unable to accurately detect the rotating instability. In addition, all four acoustic sensors capture two low frequencies, one is 24.4 Hz and the other is 9.9 Hz, and neither of these two frequencies is captured by dynamic pressure transducers, so it is unlikely that they are related to the pressure oscillations inside the compressor. Instead, the 24.4 Hz frequency may be caused by the test rig and the 9.9 Hz one is believed to be the Helmholtz oscillation of the system as it is quite close to the Helmholtz frequency.

The frequency characteristics of acoustic signals at operation point L9 (rotating stall) and L10 (mild surge) are presented in Fig. 12 and Fig. 13, respectively. As for the rotating stall operation condition, Fig. 12 shows that all four acoustic sensors, whether

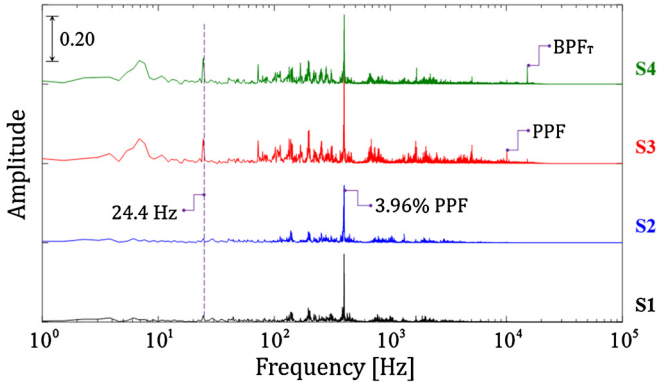

Fig. 12. Frequency characteristic of acoustic signals at "L9" (rotating stall).

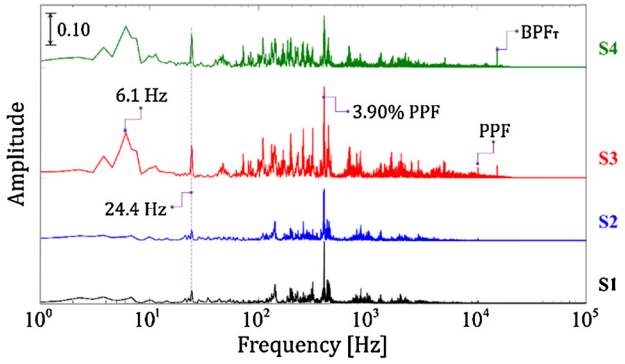

Fig. 13. Frequency characteristic of acoustic signals at "L10" (mild surge).

they are installed near the inlet pipe entrance ("S1" and "S2") or near the compressor casing ("S3" and "S4"), clearly capture the generation frequency of stall cells (3.96% PPF), and the frequency is highly agreed with that captured by dynamic pressure transducers (3.93% PPF). It is the same for mild surge operation condition. According to Fig. 13, the generation frequency of accompanied rotating stall (3.90% PPF) obviously appears in the frequency spectrum and agrees well with the pressure result (3.94% PPF). Nevertheless, the frequency of mild surge disturbance does not appear in the frequency spectrum, even though it is clearly captured by dynamic pressure transducers in both frequency domain (Fig. 6) and time domain (Fig. 9). Therefore, according to the analysis on low rotating speed (50%), the generation frequency of rotating stall could be accurately captured and distinguished by acoustic signals, but acoustic signals fail to detect the frequency of mild surge disturbance.

Unlike the dynamic pressure transducers, acoustic sensors in this investigation do not contact with the flow, and sounds generated by the flow inside the compressor need to propagate across the compressor casing or through the long inlet pipe before reaching to acoustic sensors. The acoustic signals are likely to attenuate to a quite low level after the propagation and thus it cannot be detected by acoustic sensors. In other words, the mild surge disturbances need to be strong enough so that it can be detected by acoustic sensors after the propagation process. To prove this, the mild surge point at 100% rotating speed (H5) is analyzed. As shown in Fig. 14, the pressure signal behavior in time domain indicates the amplitude is approximately 10% of the reference dynamic pressure, and there exist four mild surge cycles within 750 rotor revolutions, so the mild surge frequency at 100% rotating speed is about 18.2 Hz (the PPF at high rotating speed is 20430 Hz). In contrast, Fig. 15 shows the acoustic signal behavior of operation point "H5"in frequency domain, and the mild surge frequency (18.3 Hz) is easy to be distinguished in the frequency spectrum of

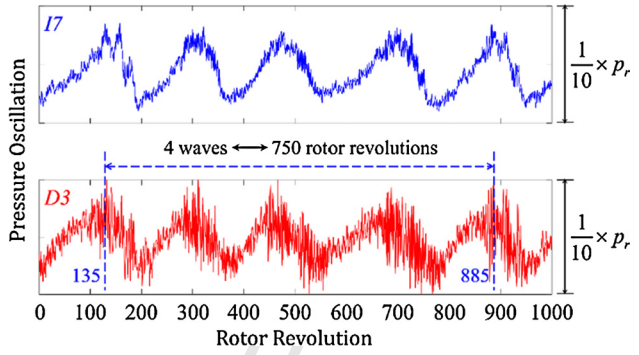

Fig. 14. Pressure signal of mild surge at 100% speed (H5) recorded by "I7" and "D3".

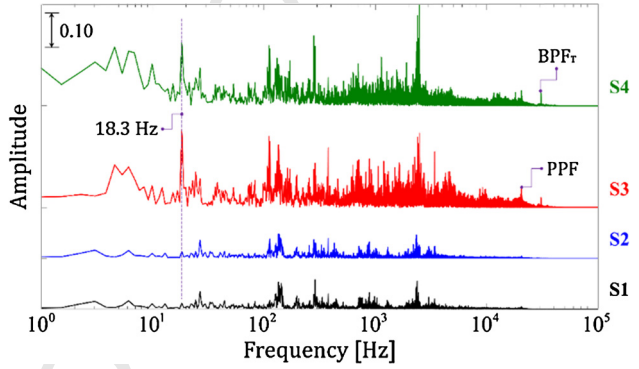

Fig. 15. Frequency characteristic of acoustic signals at "H5" (mild surge at 100% speed).

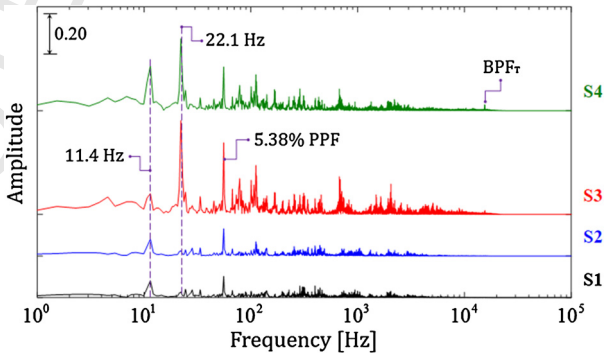

Fig. 16. Frequency characteristic of acoustic signals at "L11" (deep surge).

acoustic signals recorded by "S3" and "S4". In addition, the mild surge frequency also appears in the frequency spectrum of "S1" and "S2" with a much smaller amplitude than those of "S3" and "S4". According to equation (3), the absolute value of the reference dynamic pressure of 100% rotating speed is four times that of low rotating speeds (50%). Therefore, the amplitude of mild surge disturbance of "H5" is also four times that of "L10", thus, the acoustic signal generated by mild surge disturbance is strong enough to be detected by acoustic sensors after propagation process.

Fig. 16 shows the frequency spectrum of acoustic signals recorded at the deep surge condition of low rotating speed. The 11.4 Hz frequency is distinguishable in the frequency spectrum, and it is captured by all four acoustic sensors. The PPF of the compressor at deep surge condition of low rotating speed is approximately 10170 Hz, therefore, the 11.4 Hz frequency is about 1.12‰ of PPF. According to the analysis in Fig. 10(b), the frequency of deep surge cycles at low rotating speed is 1.11‰ PPF, which indicates that the 11.4 Hz frequency captured by acoustic sensors denotes deep surge frequency. Thus, the deep surge frequency

could be accurately captured and distinguished by acoustic signals. Additionally, it is obvious that a certain frequency, which is close to 22.4 Hz, appears in all the frequency spectrums in Fig. 11, Fig. 12, Fig. 13 and Fig. 16, so it is evident that this frequency appearing in acoustic signals is independent on operation points, and it proves again that the frequency is not caused by the flow disturbance inside the compressor, but caused by the test rig.

Throughout all the frequency analysis of acoustic signals, characteristic frequencies of instability phenomena seem more prominent in frequency spectra of "S3" and "S4", especially at mild surge condition (see Fig. 15) and deep surge condition (see Fig. 16). In addition, acoustic signals recorded by "S3" and "S4" contain much more frequency elements than those of "S1" and "S2". For example, "S3" and "S4" could capture the blade passing frequency of the turbine (BPF_T) and the PPF of the impeller, but "S1" and "S2" cannot do this. The acoustic sensors "S3" and "S4" are installed near the compressor casing, and "S1" and "S2" are installed near the inlet pipe entrance, which induces a long-distance propagation and remarkable attenuation of acoustic signals before they could be recorded by "S1" and "S2". Therefore, it is suggested to install acoustic sensors near the compressor casing to get as much information as possible.

According to the analysis above, a guideline for instability detection by acoustic measurements could be expressed as follows: acoustic measurements have the ability to detect and distinguish rotating stall, mild surge and deep surge by capturing their characteristic frequencies, and the acoustic sensor is suggested to be installed near the compressor casing. Meanwhile, analysis also points out that the characteristics of rotating instability are difficult to be distinguished via acoustic signals, and whether the mild surge could be detected significantly depends on the strength of the disturbance after the propagation process.

4. Conclusions

This paper investigates the pressure and acoustic characteristics of different instability phenomena of a centrifugal compressor and analyzes the ability of acoustic measurement to detect instabilities. Results reveal that totally four instability phenomena occur within the compressor, and they are the rotating instability, the rotating stall, the mild surge and the deep surge. The rotating instability is characterized by a broadband feature in the frequency spectrum, and the rotating stall is characterized by the generation frequency of stall cells that is approximately 4% of PPF. Both the mild surge and the deep surge are characterized by a frequency close to the Helmholtz frequency of the compression system, but the oscillation amplitude of the deep surge is much larger than that of the mild surge, and the pressure presents a wave-like shape at the mild surge condition whereas a leptokurtic waveform at the deep surge condition. According to whether the characteristic frequency appears in the frequency spectrum, the ability of acoustic measurement to detect instabilities is analyzed, and a guideline is concluded as follows: acoustic sensors are suggested to be installed near the compressor casing to capture as much information as possible, and it is found that acoustic measurement has the ability to detect and distinguish instability phenomena of rotating stall, mild surge and deep surge. This paper provides a simple, flexible and low-cost method to detect instability phenomena via acoustic measurement in the real operating environment, and it could be used for compressor products during the full life cycle as it is a non-contacting measurement and no additional manufacture is needed.

Conflict of interest statement

None declared.

Acknowledgements

This research was supported by the National Natural Science Foundation of China (Grant No. 51876097). Special thanks to Mr. Zhaoqi Yan from National Key Laboratory of Science and Technology on Aero-Engine Aero-Thermodynamics for his effort in data post-processing.

References

[1] I.J. Day, Stall, surge, and 75 years of research, J. Turbomach. 138 (1) (2016) 011001.
[2] A. Young, I. Day, G. Pullan, Stall warning by blade pressure signature analysis, J. Turbomach. 135 (1) (2013) 011033.
[3] J. Marz, C. Hah, W. Neise, An experimental and numerical investigation into the mechanisms of rotating instability, J. Turbomach. 124 (3) (2002) 367–374.
[4] R. Mailach, I. Lehmann, K. Vogeler, Rotating instabilities in an axial compressor originating from the fluctuating blade tip vortex, J. Turbomach. 123 (3) (2001) 453–460.
[5] H.W. Emmons, Compressor surge and Stall Propagation, ASME Paper No. 53-A-65, ASME, 1955.
[6] C.S. Tan, I.J. Day, S. Morris, A. Wadia, Spike-type compressor stall inception, detection, and control, Annu. Rev. Fluid Mech. 42 (2010) 275–300.
[7] H.D. Vo, C.S. Tan, E.M. Greitzer, Criteria for spike initiated rotating stall, J. Turbomach. 130 (1) (2008) 011023.
[8] J.M. Haynes, G.J. Hendricks, A.H. Epstein, Active Stabilization of Rotating Stall in a Three-Stage Axial Compressor, ASME Paper No. 93-GT-346, ASME, 1993.
[9] J.D. Paduano, E.M. Greitzer, A.H. Epstein, Compression system stability and active control, Annu. Rev. Fluid Mech. 33 (1) (2001) 491–517.
[10] E.M. Greitzer, Surge and rotating stall in axial flow compressors—part II: experimental results and comparison with theory, J. Eng. Gas Turbines Power 98 (2) (1976) 199–211.
[11] N.A. Cumpsty, Compressor Aerodynamics, Krieger Publishing Company, Malabar, FL, 2004.
[12] E.M. Greitzer, The stability of pumping systems—the 1980 Freeman scholar lecture, J. Fluids Eng. 103 (2) (1981) 193–242.
[13] C. Li, S. Xu, Z. Hu, Experimental study of surge and rotating stall occurring in high-speed multistage axial compressor, Proc. Eng. 99 (2015) 1548–1560.
[14] X. Zheng, Liu A. Phenomenon, and mechanism of two-regime-surge in a centrifugal compressor, J. Turbomach. 137 (8) (2015) 081007.
[15] X. Zheng, Z. Sun, T. Kawakubo, H. Tamaki, Experimental investigation of surge and stall in a turbocharger centrifugal compressor with a vaned diffuser, Exp. Therm. Fluid Sci. 82 (2017) 493–506.
[16] Z. Sun, X. Zheng, T. Kawakubo, Experimental investigation of instability inducement and mechanism of centrifugal compressors with vaned diffuser, Appl. Therm. Eng. 133 (2018) 464–471.
[17] D. Alone, S. Kumar, M. Shobhavathy, J. Mudipalli, A. Pradeep, S. Ramamurthy, V. Iyengar, Experimental assessment on effect of lower porosities of bend skewed casing treatment on the performance of high speed compressor stage with tip critical rotor characteristics, Aerosp. Sci. Technol. 60 (2017) 193–202.
[18] C. Brandstetter, H.P. Schiffer, PIV measurements of the transient flow structure in the tip region of a transonic compressor near stability limit, J. Glob. Power Propuls. Soc. 2 (2018) 303–316.
[19] A. Zamiri, B. Lee, J. Chung, Numerical evaluation of transient flow characteristics in a transonic centrifugal compressor with vaned diffuser, Aerosp. Sci. Technol. 70 (2017) 244–256.
[20] I. Shahin, M. Alqaradawi, M. Gadala, O. Badr, On the aero acoustic and internal flows structure in a centrifugal compressor with hub side cavity operating at off design condition, Aerosp. Sci. Technol. 60 (2017) 68–83.
[21] G. Pullan, A.M. Young, I.J. Day, E.M. Greitzer, Z.S. Spakovszky, Origins and structure of spike-type rotating stall, J. Turbomach. 137 (5) (2015) 051007.
[22] E. Munari, G. D'Elia, M. Morini, E. Mucchi, M. Pinelli, P.R. Spina, Experimental Investigation of Vibrational and Acoustic Phenomena for Detecting the Stall and Surge of a Multistage Compressor, ASME Paper No. GT2017-64894, ASME, 2017.
[23] E.M. Greitzer, Surge and rotating stall in axial flow compressors—part I: theoretical compression system model, J. Eng. Gas Turbines Power 98 (2) (1976) 190–198.